

# Manganese and color cycles in Arctic Ocean sediments constrain Pleistocene chronology

Martin Jakobsson Department of Geology and Geochemistry, Stockholm University, S-106 91 Stockholm, Sweden

Reidar Løvlie Institute of Solid Earth Physics, Allégatan 41, N-5007, Bergen, Norway

Hakam Al-Hanbali

Eve Arnold

Jan Backman

Magnus Mörrth

Department of Geology and Geochemistry, Stockholm University, S-106 91 Stockholm, Sweden

## ABSTRACT

**Sequential variations in manganese (Mn) content and color of deep-sea sediments retrieved from the Lomonosov Ridge (87°N) in the central Arctic Ocean apparently mimic low-latitude  $\delta^{18}\text{O}$  glacial-interglacial cyclicity, thereby providing stratigraphic information that together with biostratigraphic data permit the construction of a detailed chronological model. Correlation of this Mn and color chronology to established apparent Brunhes-age estimates of geomagnetic excursions reveals a remarkable fit between these two independently derived time scales. The Mn and color cycles probably provide paleoenvironmental information about material fluxes in the Arctic Ocean over the past 1 m.y. We suggest that the primary source for the observed manganese variations in our sediment core is northern Siberia, which has extensive peat bogs and boreal forests. These Siberian source areas could operate in an off and on mode tuned to Pleistocene glacial and interglacial periods. Contrasts in ventilation of Arctic Ocean waters during interglacial-glacial cycles probably could also enhance the observed Mn and color variability.**

**Keywords:** Arctic Ocean, chronology, manganese, cyclicity, sediments, color.

## INTRODUCTION

The Cenozoic paleoenvironmental development of the central Arctic Ocean is still largely unknown because of a lack of well-dated long deep-sea sediment cores that record the history of pelagic sedimentation in this region. A problem specific to Arctic Ocean sediments is the difficulty involved in establishing accurate age-depth relationships in the existing sediment cores (Thiede et al., 1990; Darby et al., 1997). Poor preservation of calcareous microfossil faunas and floras in Arctic cores precludes application of conventional biostratigraphic and isotopic paleoceanographic dating techniques. Therefore, chronological models have largely relied on paleomagnetic reversal stratigraphy (Steuerwald et al., 1968; Clark, 1970; Aksu, 1985; Witte and Kent, 1988; Poore et al., 1993; Schneider et al., 1996; Phillips and Grantz, 1997) and dating methods such as  $^{10}\text{Be}$  (Eisenhauer et al., 1994; Aldahan et al., 1997), amino acids (Sejrup et al., 1984; Macku and Aksu, 1986), or lithostratigraphy (Clark et al., 1980), and interpolation between these and  $^{14}\text{C}$  dating (Poore et al., 1994; Stein et al., 1994; Spielhagen et al., 1997). Paleomagnetic reversal stratigraphy relies on the interpretation of zones with negative inclination that represent either complete reversals or partial excursions of the geomagnetic field. Reversals occur over time scales of a few hundred thousand years, whereas excursions commonly last <10 k.y. (Jacobs, 1994); thus different interpretations of the magnetic boundaries may result in inferred sedimentation rates that differ by at least one order of magnitude (Frederichs, 1995). Other methods have also shown that sedimentation may vary widely with location and stratigraphic depth (Clark et al., 1980; Darby et al., 1997; Huh et al., 1997; Nørgaard-Pedersen et al., 1998)

We present a chronology of an Arctic Ocean core (96/12-1pc) based on biostratigraphic data combined with an analytical approach that uti-

lizes Mn and color cycles as a proxy for paleoclimatic variability. We postulate that the Mn and color variability mimics low-latitude oxygen isotope oscillations, and we have therefore assigned ages to the sediment based on correlation with this low-latitude record. The resulting Mn and color time scale shows a close correlation with an independent paleomagnetic chronology of the core derived from inferred correlation of geomagnetic inclination excursions with Brunhes excursion ages (Langereis et al., 1997).

## STUDY SITE AND METHODS

The 722-cm-long piston core was retrieved in 1996 from the crest of the Lomonosov Ridge at 87°05.9'N, 144°46.4'E, 1003 m water depth (Fig. 1). The core consists of horizontally bedded silty clay and clay; the top 3 cm of oxidized dark brown silty clay was disturbed by the coring process. Between 3 and 115 cm, the sediments consist of light brown to light yellowish-brown, mottled clayey silt with faint horizontal color banding. A homogeneous dark gray silty clay unit occurs between 115 and 163 cm; this unit has a sharp contact with an underlying olive to light brown clay (163–186 cm). The olive to light brown clay grades into a coarse-grained, light gray-brown sandy clay that occurs from 186 to 191 cm. There is a sharp contact between this sandy clay and the underlying, thin (1 cm) olive-gray clay, which in turn has a sharp contact with another 1-cm-thick, light brown clay. Between 193 and 722 cm, the sediment consists of dark brown to medium brown oxidized bioturbated

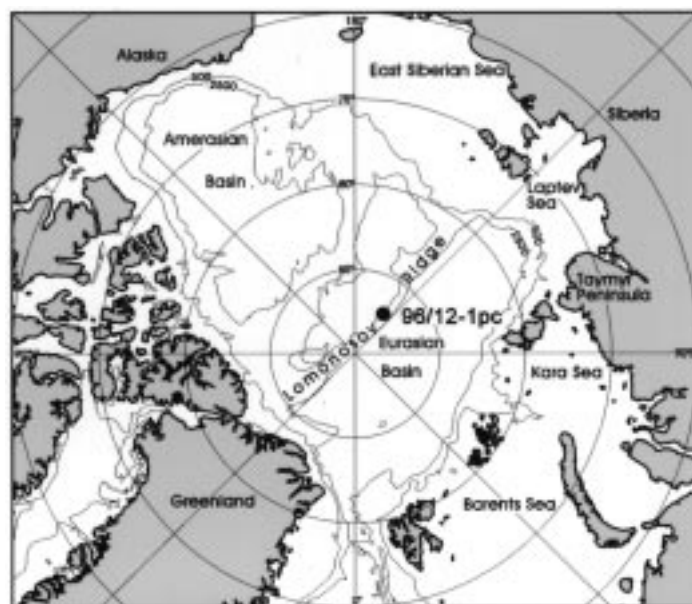


**Figure 1.** Location map showing site of core 96/12-1pc on crest of Lomonosov Ridge in central Arctic Ocean.

Data Repository item 20008 contains additional material related to this article.

clay units alternating with light brown clay (Fig. 2).<sup>1</sup> The dark brown units below 193 cm occur in a cyclic fashion, are 2–14 cm thick, and are lithologically similar to the uppermost 3 cm of the core. The lithology of a 28-cm-long trigger weight core taken at the same site contains two dark brown oxidized silty clay units that are not recognized in the piston core, indicating that the uppermost 15–20 cm were not recovered in core 96/12-1pc.

The core was digitally imaged using an image capturing system mounted in a configuration conforming to the Commission Internationale de l'Eclairage 45/0 standard for viewing and illumination (Wyszecki and Stiles, 1982). The split core sections were imaged at 30 cm intervals with 10 cm overlap. A continuous core image was assembled by creating a digital mosaic of the 30 cm intervals at a resolution of 4.8 pixels/mm. Discrete samples for paleomagnetic measurements were continuously taken in the center of the split core with 6.2 cm<sup>3</sup> cubic plastic boxes, following the procedures of Løvlie et al. (1986) in order to minimize disturbance; 1.5-m-long U-channels (2 × 2 cm) were also analyzed, taken from the center of the split core. The dimension of a 6.2 cm<sup>3</sup> cubic plastic box is 1.55 × 2 × 2 cm of which 1.55 × 2 cm (vertically × horizontally) comprises the area at the split core surface. The core diameter is 8.8 cm. Paleomagnetic measurements and progressive alternating field demagnetization (maximum 60 mT) were obtained at 1 cm intervals with the 2G DC SQUID system at Gif-sur-Yvette (Weeks et al., 1993). Major and trace elements were determined for 121 samples using ion coupled plasma atomic emission spectroscopy (Walsh, 1997). For this purpose, we used the samples from the discrete magnetic analyses. The samples were freeze dried and homogenized, and ~100 mg of powder were fused and dissolved following the procedures of Burman et al. (1978). Triplicate analyses were made on a Spectroflame Modula spectrophotometer. Smear slides for calcareous nannofossil counts were prepared at 5 cm intervals. In each smear slide, we examined 50 fields of view between crossed nicols at 1250× magnification using a view-field diameter of 0.17 mm, and the taxonomy of Gard and Backman (1990).

## RESULTS AND DISCUSSION

Calcareous nannofossils were observed in the upper 285 cm of the core. Occurrences of *Gephyrocapsa* spp. and *Emiliania huxleyi* were used to identify oxygen isotope stages (OIS) 1 and 5 (Fig. 3). *Emiliania huxleyi* evolved during oxygen isotope stage (OIS) 8 (Thierstein et al., 1977), but biostratigraphy indicates that this species did not appear in the Arctic Ocean until OIS 5 (Gard and Backman, 1990; Gard, 1993). Nannofossils in the short trigger weight core represent OIS 1, demonstrating that the dark brown oxidized clay represents interglacial sedimentation. Abundance peaks of *G. muelleriae*-type geophyrocapsids and the presence of *E. huxleyi*, which coincide with dark brown lithologic intervals centered at 195 and 220 cm, are thus interpreted to represent OIS 5.1 and OIS 5.5, respectively (Fig. 3). Another dark brown interval at ~204 cm contains these two taxonomic categories as well as a specimen of *Coccolithus pelagicus* and is therefore assigned to OIS 5.3.

Manganese concentrations (expressed as MnO) range between 0.03 and 1.34 wt%. Manganese peaks clearly coincide with the dark to medium brown bioturbated units below 193 cm (Figs. 2 and 3). A relationship between manganese concentration and color values (red, green, and blue, RGB) was determined by multiple regression analysis. Red, green, and blue values were averaged over the same intervals as the samples taken for chemical analyses, thus they correspond to the mean color of the chemically analyzed sample. This multiple regression analysis yielded a correlation coefficient of  $r^2 \sim 0.63$ . A transfer function for estimating manganese concentrations from red, green, and blue values was then derived for the lower part

<sup>1</sup>Data Repository item 20008—a high-resolution digital image of the complete core 96/12-1pc and the trigger weight core taken at the same site, a plot showing the data of multiple regression, MnO raw data and red, green, blue values used to derive equation 1, and predicted MnO values and error estimates—is available on request from Documents Secretary, GSA, P.O. Box 9140, Boulder, CO 80301, editing@geosociety.org, or at www.geosociety.org/pubs/drpint.htm.

of the core. An optimal linear model was calculated introducing a vector for the normalized B (B/[R + B + G]) into the multiple regression, which improved the correlation to  $r^2 \sim 0.75$ . The transfer function (equation 1; see footnote 1) was used to estimate manganese concentrations at 0.5 cm intervals below 193 cm core depth (Figs. 2 and 3).

$$\text{MnO (wt\%)} = -23.58 + 0.0904R + 0.0659G - 0.2299B + 92.68(B/[R + G + B]), \quad (1)$$

where R is the red, G the green, and B the blue color values retrieved from the RGB color image of the core

Anomalously shallow paleomagnetic inclinations in the uppermost 20 cm are attributed to high water content sediment deformation during coring. Steep inclinations below 200 cm define 11 intervals of reversed polarity, in general agreement with neighboring core PS2185-6 (Frederichs, 1995). Lacking independent age control, Frederichs proposed two alternative interpretations of the polarity stratigraphy in PS2185-6: excursions or reversals. Adopting the reversal alternative, core PS2185-6 would extend to the Gilbert chron at 4.8 Ma. However, normal polarity intervals occupy 75% of the core stratigraphy, which is significantly larger than the 40% proportion of normal polarity suggested by the geomagnetic polarity time scale for the past 4.8 m.y. (Cande and Kent, 1995). In addition, grain-size analyses do not demonstrate the cyclical variability observed in the Mn and color record below 193 cm in the core, eliminating variable input of ice-rafted debris as a cause of the highly variable sedimentation rates that the magnetic reversal model yields in this interval. On the basis of these considerations and our biostratigraphy, we suggest that the reversed polarity zones represent excursions in both cores PS2185-6 and 96/12-1pc. The absence of excursions at and above OIS 5.5 is attributed to either postdepositional realignment of magnetic grains within the significantly coarser sediments in the upper part of the core (Fig. 3), or to unresolved overprints.

We suggest that the dark to medium brown units characterized by increased manganese concentrations that occur in a cyclic fashion in core 96/12-1pc reflect oxygenated water mass conditions at ~1 km depth during interglaciations. Our reasons are: (1) four short intervals containing interglacial occurrences of indigenous Pleistocene and Holocene calcareous nannofossils in the upper 285 cm of the core all occur in dark brown sediment units; (2) the dark brown units are mottled, indicating bioturbation, increased biological activity, and ventilated waters at ~1 km depth; (3) the dark brown units contain enhanced manganese concentrations, which are indicative of oxidizing conditions.

Manganese in marine sediments may be precipitated from hydrothermal solutions and seawater, as well as being precipitated diagenetically (Hein et al., 1992), resulting in layered concentration differences (Froelich et al., 1979). The presence of 19 lithologic cycles in cores from the Northwind Ridge in the Amerasian basin was recently interpreted to represent variable states of oxygenation driven by glacial-interglacial changes during the early Pleistocene through Holocene (Phillips and Grantz, 1997). Interglaciations are represented by units with dark yellowish-brown mud containing relatively higher concentrations of FeMn micronodules. This supports our interpretation that Mn-rich layers may be associated with interglaciations when periods with diminished sea ice enhanced the ventilation of intermediate deep Arctic Ocean waters. Possible links between manganese concentrations in Arctic Ocean sediments and glacial-interglacial cycles have been discussed (e.g., Boström, 1970, and Polyak, 1986).

An age model for the upper 220 cm of core 96/12-pc has been constructed based on nannofossil biostratigraphy. Below this depth, OIS ages are inferred from correlation of sediment Mn and color cycles (Fig. 3), using a low-latitude  $\delta^{18}\text{O}$  stack (Bassinot et al., 1994). OIS stages 3.1 and 3.3 are assigned to manganese peaks that apparently did not correlate to dark brown sediment units. The stratigraphically deepest Mn and color cycle is centered at 626.5 cm and has been assigned to OIS 21.5 (858 ka). This age model yields sedimentation rates with two distinct slopes: one

encompassing OIS 1 through OIS 4 (2.8 cm/k.y.), and the other encompassing OIS 5 through OIS 21.5 (0.5 cm/k.y.). We have correlated core 96/12-1pc to neighboring core PS2185-6 using physical property data (polarity pattern, grain size, bulk density, and magnetic susceptibility). Our age model suggests a Pleistocene age for core PS2185-6, supporting Frederichs' excursion age model scenario rather than the polarity zone model (Frederichs, 1995; Spielhagen et al., 1997).

The Mn- and color-derived time scale is independently supported if we assign Brunhes ages (Langereis et al., 1997) to apparent geomagnetic excursions of core 96/12-1pc (Fig. 3, left side and black squares). However, the reversal pattern below the inferred Brunhes-Matuyama boundary cannot be correlated to the geomagnetic polarity time scale without introducing major discontinuities in sediment accumulation rates. This apparent anomaly cannot be resolved until further independent chronologies are developed.

Two different processes may be invoked to create the observed cyclic pattern of manganese concentration. (1) Climatic forcing of the transport of source material from northern Siberia, e.g., rivers draining peat areas, lake systems, and boreal forests, bringing large quantities of manganese to the central Arctic Ocean today (Pontér et al., 1992; Kassens et al., 1998). Northern Siberia represents a huge source for manganese to the Arctic Ocean, and this source area has been active through its rivers during interglacials and comparatively inactive during glacials. (2) The relative degree of ventilation of Arctic Ocean waters also was driven by glacial-interglacial contrasts (Phillips and Grantz, 1997), which would enhance the precipitation of manganese during interglacials because of higher bottom water oxygen concentrations.

The cause of the sharp change in sedimentation rate at about the OIS 5-OIS 4 transition remains speculative (Fig. 3), although our data set suggests

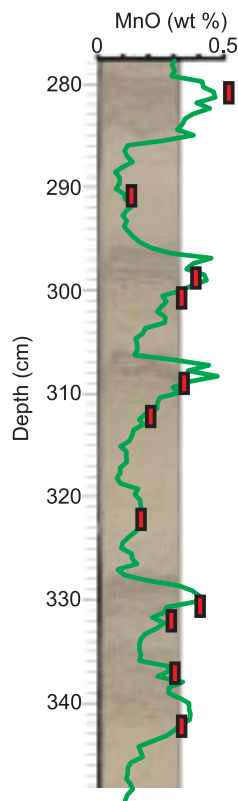


Figure 2. Digitally photographed core section showing distinct color cycles. Red bars represent MnO contents of chemically ion coupled plasma atomic emission spectroscopy analyzed samples; green line represents predicted MnO contents derived from equation 1.

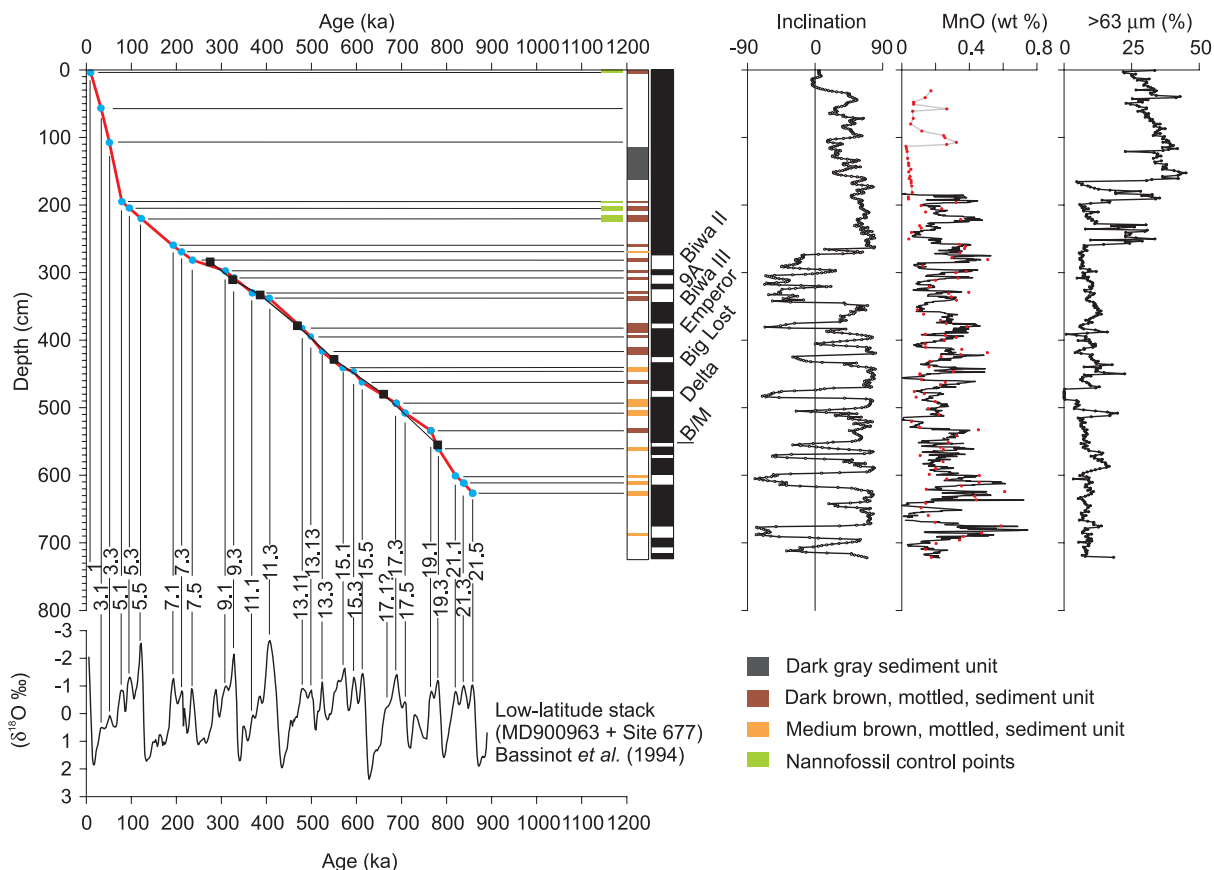


Figure 3. Age model for core 96/12-1pc derived from nannofossil biostratigraphy and manganese and color cycles correlated to low-latitude  $\delta^{18}\text{O}$  stack (Bassinot et al., 1994). Black boxes in age/depth plot represent Brunhes excursions, and blue filled circles represent manganese and color cycles correlated to oxygen isotope stages. Color cycles and names of geomagnetic excursions (Langereis et al., 1997) are indicated in two columns on right side of age-depth plot. Red circles in MnO content plot represent chemically ion coupled plasma atomic emission spectroscopy analyzed samples; black line represents predicted MnO contents derived from red, green, and blue color values.

a possible link between sedimentation rate and grain size. Coarser grain sizes occur during glacials from OIS 6 and onward; our chronology model, however, cannot resolve an increase in sedimentation rate within OIS 6. Correlation to core PS2185-6 suggests a concomitant increase in concentration of smectite, which Spielhagen et al. (1997) interpreted to reflect the initiation of large-scale glaciation in northern Siberia at 0.7 Ma. Our age model indicates an age of about 0.15 Ma for this event.

#### ACKNOWLEDGMENTS

Core 96/12-1pc was collected during the Arctic Ocean 1996 expedition, which was organized and financed by the Swedish Polar Research Secretariat. We thank C. Kissel and A. Mazaud for assistance in running the magnetometer at Gif-sur-Yvette. Heather Renyck and Marianne Ahlborn analyzed the grain size in the core. John Imbrie made helpful suggestions on an earlier version of the manuscript. We are grateful for constructive reviews provided by Julie Brigham-Grette and an anonymous reader. The project was financed by the Swedish Natural Science Research Council.

#### REFERENCES CITED

- Aksu, A. E., 1985, Paleomagnetic stratigraphy of CESAR cores, in Jackson, H. R., et al., eds., Initial geological report on CESAR—The Canadian Expedition to study the Alpha Ridge, Arctic Ocean: Geological Survey of Canada Paper 84-22, p. 101–114.
- Aldahan, A. A., Shi Ning, Possnert, G., Backman, J., and Boström, K., 1997, <sup>10</sup>Be records from sediments of the Arctic Ocean covering the past 350 ka: Marine Geology, v. 144, p. 144–162.
- Bassinot, F. C., Labeyrie, L. D., Vincent, E., Quidelleur, X., Shackleton, N. J., and Lancelot, Y., 1994, The astronomical theory of climate and the age of the Brunhes-Matuyama magnetic reversal: Earth and Planetary Science Letters, v. 126, p. 91–108.
- Boström, K., 1970, Deposition of manganese rich sediments during glacial periods: Nature, v. 226, p. 629–630.
- Burman, J. O., Pontér, C., and Boström, K., 1978, Metaborate digestion procedure for inductively coupled plasma-optical emission spectrometry: Analytical Chemistry, v. 50, p. 679–680.
- Cande, S. C., and Kent, D. V., 1995, Revised calibration of the geomagnetic polarity timescale for the Late Cretaceous and Cenozoic: Journal of Geophysical Research, v. 100, p. 6093–6095.
- Clark, D. L., 1970, Magnetic reversals and sedimentation rates in the Arctic Basin: Geological Society of America Bulletin, v. 81, p. 3129–3134.
- Clark, D. L., Whitman, R. R., Morgan, K. A., and Mackay, S. D., 1980, Stratigraphy and glacial-marine sediments of the Amerasian Basin, central Arctic Ocean: Geological Society of America Special Paper 181, p. 1–57.
- Darby, D. A., Bischof, J. F., and Jones, G. A., 1997, Radiocarbon chronology of depositional regimes in the western Arctic Ocean: Deep Sea Research, v. 55, p. 1745–1757.
- Eisenhauer, A., Spielhagen, R. F., Frank, M., Hentzschel, G., Mangini, A., Kubik, P. W., Ditttrich-Hannen, B., and Billen, T., 1994, <sup>10</sup>Be records of sediment cores from high northern latitudes: Implications for environmental and climate changes: Earth and Planetary Science Letters, v. 124, p. 171–184.
- Frederichs, T., 1995, Regional and temporal variations of rock magnetic parameters in Arctic marine sediments: Berichte zur Polarforschung, no. 164, p. 1–212.
- Froelich, P. N., Klinkhammer, G. P., Bender, M. L., Luedtke, N. A., Heath, G. R., Cullen, D., and Dauphin, P., 1979, Early oxidation of organic matter in pelagic sediments of the eastern equatorial Atlantic: Suboxic diagenesis: Geochimica et Cosmochimica Acta, v. 43, p. 1075–1090.
- Gard, G., 1993, Late Quaternary coccoliths at the North Pole: Evidence of ice-free conditions and rapid sedimentation in the central Arctic Ocean: Geology, v. 21, p. 227–230.
- Gard, G., and Backman, J., 1990, Synthesis of Arctic and subarctic coccolith biochronology and history of North Atlantic drift water influx during the last 500,000 years, in Bleil, U., and Thiede, J., eds., Geological history of the polar oceans: Arctic versus Antarctic: Dordrecht, Kluwer, NATO ASI Series C, p. 417–436.
- Hein, J. R., Bohron, W. A., Schulz, M. S., Noble, M., and Clague, D. A., 1992, Variations in the fine-scale composition of a central Pacific ferromanganese crust: Paleoclimatological implications: Paleoceanography, v. 7, p. 63–77.
- Huh, C. A., Piasias, N. G., Kelly, J. M., Maiti, T. C., and Grantz, A., 1997, Natural radionuclides and plutonium in sediments from western Arctic Ocean: Sedimentation rates and pathways of radionuclides: Deep Sea Research, v. 44, p. 1725–1744.
- Jacobs, J. A., 1994, Reversals of the earth's magnetic field: Cambridge, Cambridge University Press, p. 1–346.
- Kassens, H., Dmitrenko, I., Rachold, V., Thiede, J., and Timokhov, L., 1998, Russian and German scientists explore the Arctic's Laptev Sea and its climate system: Eos (Transactions, American Geophysical Union), v. 79, p. 317, 322–323.
- Langereis, C. G., Dekkers, M. J., de Lange, G. J., Paterne, M., and van Santvoort, P. J. M., 1997, Magnetostratigraphy and astronomical calibration of the last 1.1 Ma from an eastern Mediterranean piston core and dating of short events in the Brunhes: Geophysical Journal International, v. 129, p. 75–94.
- Løvlie, R., Markussen, B., Sejrup, H. P., and Thiede, J., 1986, Magnetostratigraphy in three Arctic Ocean sediment cores; arguments for magnetic excursions within oxygen-isotope stage 2–3: Physics of the Earth and Planetary Interiors, v. 43, p. 173–184.
- Macku, S. A., and Aksu, A. E., 1986, Amino acid epimerization in planktonic foraminifera suggest slow sedimentation rates for Alpha Ridge, Arctic Ocean: Nature, v. 322, p. 730–732.
- Nørgaard-Pedersen, N., Spielhagen, R., Thiede, J., and Kassens, H., 1998, Central Arctic surface ocean environment during the past 80,000 years: Paleoceanography, v. 13, p. 193–204.
- Phillips, R. L., and Grantz, A., 1997, Quaternary history of sea ice and paleoclimate in the Amerasia basin, Arctic Ocean, as recorded in cyclical strata of Northwind Ridge: Geological Society of America Bulletin, v. 109, p. 1101–1115.
- Polyak, L. V., 1986, New data on microfauna and stratigraphy of bottom sediments of the Mendeleev Ridge, Arctic ocean, in Andreyev, S. I., et al., eds., The genesis of sediments and formation of nodules in the ocean: Leningrad, Sevmoregeologia, p. 40–50.
- Pontér, C., Ingri, J., and Boström, K., 1992, Geochemistry of manganese in the Kalix river, northern Sweden: Geochimica et Cosmochimica Acta, v. 56, p. 1485–1494.
- Poore, R. Z., Phillips, R. L., and Rieck, H. J., 1993, Paleoclimate record for Northwind Ridge, western Arctic Ocean: Paleoceanography, v. 8, p. 149–159.
- Poore, R. Z., Ishman, S. E., Phillips, R. L., and McNeil, D., 1994, Quaternary stratigraphy and paleoceanography of the Canada Basin, western Arctic Ocean: U.S. Geological Survey Bulletin 2080, p. 1–32.
- Schneider, D. A., Backman, J., Curry, W. B., and Possnert, G., 1996, Paleomagnetic constraints on sedimentation rates in eastern Arctic Ocean: Quaternary Research, v. 46, p. 62–71.
- Sejrup, H. P., Gifford, H. M., Brigham-Grette, J., Løvlie, R., and Hopkins, D., 1984, Amino acid epimerization implies rapid sedimentation rates in Arctic ocean cores: Nature, v. 310, p. 772–775.
- Spielhagen, R. F., Bonani, G., Eisenhauer, A., Frank, M., Frederichs, T., Kassens, H., Kubik, P. W., Mangini, A., Nørgaard-Pedersen, N., Nowaczyk, N. R., Schper, S., Stein, R., Thiede, J., Tiedemann, R., and Wahsner, M., 1997, Arctic Ocean evidence for late Quaternary initiation of northern Eurasian ice sheets: Geology, v. 25, p. 783–786.
- Stein, R., Nam, S. I., Schubert, C., Vogt, C., Futterer, D., and Heinemeier, J., 1994, Last deglaciation event in the eastern central Arctic Ocean: Science, v. 264, p. 692–695.
- Steuerwald, B. A., Clark, D. L., and Andrew, J. A., 1968, Magnetic stratigraphy and faunal patterns in Arctic Ocean sediments: Earth and Planetary Science Letters, v. 5, p. 79–85.
- Thiede, J., Clark, D. L., and Herman, Y., 1990, Late Mesozoic and Cenozoic paleoceanography of the northern polar oceans, in Grantz, A., et al., eds., The Arctic Ocean region: Boulder, Colorado, Geological Society of America, Geology of North America, v. L, p. 427–458.
- Thierstein, H. R., Geitzenauer, K. R., Molino, B., and Shackleton, N. J., 1977, Global synchronicity of late Quaternary coccolith datum levels: Validation by oxygen isotopes: Geology, v. 5, p. 400–404.
- Walsh, J. N., 1997, Inductively coupled plasma-atomic emission spectrometry (ICP-AES), in Gill, R., ed., Modern analytical geochemistry: Singapore, Longman Publications, p. 41–66.
- Weeks, R., Laj, C., Endignoux, L., Fuller, M., Roberts, A., Manganne, R., Blanchard, E., and Goree, W., 1993, Improvements in long-core measurement techniques: Applications in paleomagnetism and paleoceanography: Geophysical Journal International, v. 114, p. 651–662.
- Witte, W. K., and Kent, D. V., 1988, Revised magnetostratigraphies confirm low sedimentation rates in Arctic Ocean cores: Quaternary Research, v. 29, p. 43–53.
- Wyszecki, G., and Stiles, W. S., 1982, Color science: Concepts and methods, quantitative data and formulae: New York, Wiley, p. 1–950.

Manuscript received May 4, 1999

Revised manuscript received September 8, 1999

Manuscript accepted September 15, 1999